Are high-temperature superconductors exotic?

High-temperature superconductivity in the copper oxides, first discovered twenty years ago, has led researchers on a wide-ranging quest to understand and use this new state of matter. From the start, these materials have been viewed as 'exotic' superconductors, for which the term exotic can take on many meanings. The breadth of work that has taken place reflects the fact that they have turned out to be exotic in almost every way imaginable. They exhibit new states of matter (*d*-wave superconductivity, charge stripes), dramatic manifestations of fluctuating superconductivity, plus a key inspiration and testing ground for new experimental and theoretical techniques.

D. A. BONN

Department of Physics and Astronomy, University of British Columbia, Vancouver, British Columbia, V6T 1Z1, Canada

e-mail: bonn@phas.ubc.ca

For decades, the behaviour of electrons in crystalline solids has been understood by considering a single non-interacting electron in a periodic lattice of ions. The copper oxides are a spectacular case where interactions between the electrons are so important that they lead to phenomena not seen in simple metals, semiconductors and insulators. At compositions for which single-electron theory would predict a good metal, these materials are instead antiferromagnetic Mott insulators owing to the strong interactions between electrons. With slight chemical modifications they exhibit high-temperature superconductivity, charge ordering and a host of anomalous electronic properties. They also display critical behaviour, with order that fluctuates spatially through a sample and also as a function of time. All of these phenomena are very susceptible to defects and small changes in chemical composition and structure, which presents a challenge in materials comprising four, five, even six or more elements. Gaining control over these materials issues has ushered in an era of condensed-matter physics in which transition metal oxides and other complex compounds are a central route to new physics, and inspires ingenious experimental techniques and theoretical ideas.

FROM QUANTUM MAGNET TO SUPERCONDUCTOR

High-temperature superconductivity arises in a family of layered copper oxides that all feature weakly coupled square-planar sheets of CuO_2, shown in Fig. 1. The first feature that drew attention to these materials was Bednorz and Müller's discovery in 1986 of a superconducting phase with a record-breaking critical temperature T_c near 29 K in $La_{2-x}Ba_xCuO_{4+\delta}$ (ref. 1). In just a year of feverish work, T_c leapt past the boiling point of liquid nitrogen with the discovery[2] of $YBa_2Cu_3O_{6+x}$ and later reached its highest value of 138 K in Tl-doped $HgBa_2Ca_2Cu_3O_{8+\delta}$ (ref. 3). In retrospect, the transition to such a range of T_c was the first sign that a new kind of state had been discovered. A further surprise was that it had been found in a family of oxides, very poor metals with a low density of free charge carriers. The previous record-breakers were intermetallic compounds, whose high values of T_c come from a high density of carriers bound into pairs by a strong interaction with lattice vibrations. In the 1970s, when improvements to the T_c of intermetallic compounds had petered out, other types of superconductors were being discovered that had rather high T_c values for their relatively low carrier density. A T_c of 13 K was found for $BaPb_{1-x}Bi_xO_3$, an oxide alloy with features akin to the copper oxides: a complex structural and electronic phase diagram in an oxide that could be tuned from an insulator to a low-carrier-density metal[4].

The phase diagram resulting from tuning the doping of CuO_2 planes is shown schematically in Fig. 2. Correlation effects are most apparent at compositions with one carrier per Cu atom (half-filling), where strong Coulomb repulsion yields a Mott insulator in which the motion of the charges is impeded by the high energy cost of placing two electrons on one Cu site. For a range of either hole or electron doping (removing or adding carriers), the Mott insulator is antiferromagnetic, an ordered state that is as important to the field as the presence of superconductivity. The copper oxides joined other families of superconductors, such as the heavy fermion and organic materials, which have antiferromagnetism near, or coincident with,

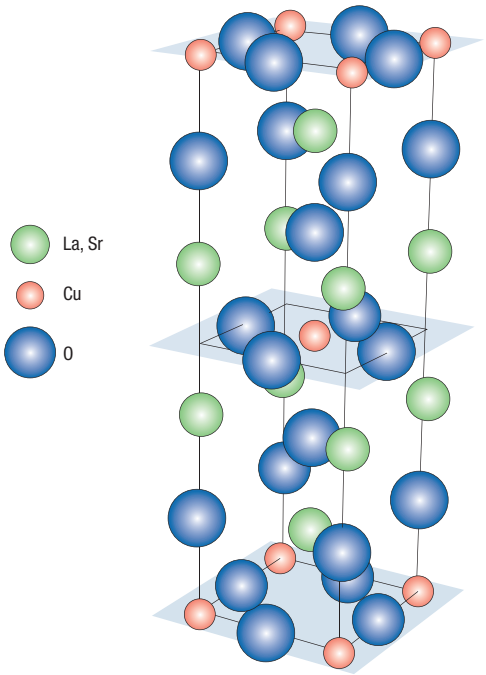

Figure 1 Crystal structure of $La_{2-x}Sr_xCuO_{4+\delta}$. The basic building block is a perovskite structure consisting of the CuO_6 octahedron seen in the centre of the unit cell, surrounded by eight La ions. The CuO_6 octahedra are elongated, giving rise to a layered structure with quasi-two-dimensional CuO_2 sheets, which are the common feature of all high-temperature superconductors. In this particular cuprate, a rocksalt-structured layer is stacked in between the perovskite cells, but there are many variations that give rise to different families of high-temperature superconductors. In $La_{2-x}Sr_xCuO_{4+\delta}$, Sr substitution for La, or the addition of interstitial oxygen, changes the carrier concentration on the CuO_2 planes, drastically altering the electronic properties of this compound.

superconductivity. When these two states are found together in one phase diagram, the possibility arises that the superconductivity is driven by magnetic interactions between carriers rather than the conventional mechanism of exchange of lattice vibrations. This had a clear precedent in ^{3}He, whose superfluid state comes from pairing mediated by spin fluctuations. A similar mechanism was under consideration for exotic families such as the heavy-fermion superconductors[5,6].

Whatever the superconducting mechanism might be, a new family of quantum magnets had been discovered, built from the rare circumstance of spin-1/2 ions in a quasi-two-dimensional square-planar array. The initial excitement stemmed in part from the possibility of discovering a spin-liquid phase. P. W. Anderson proposed that quantum fluctuations might disorder the antiferromagnetic phase, allowing the emergence of a resonating valence bond state in which the spins form a liquid of singlet pairs[7]. This provides a close link between superconductivity and magnetism by suggesting that pairing is already a feature of the materials at half-filling. However, the materials turned out to be antiferromagnets, not spin liquids, at half-filling[8,9]. Interactions between the electrons give rise to an antiferromagnetic arrangement of spins in the CuO_2 planes, with a three-dimensional magnetic transition controlled by the weaker coupling between planes. This antiferromagnetic state has been explored in detail with neutron scattering, which can measure both the spin structure of a magnet and its excitations. The magnetic order manifests itself as magnetic Bragg peaks at $[\pm\pi/a, \pm\pi/a]$ where a is the lattice spacing. When holes are added to the CuO_2 planes the antiferromagnetic transition is rapidly suppressed and a superconducting state emerges. The superconducting T_c rises with increasing hole doping through the underdoped regime, reaches a peak (optimal doping) and then falls away again at higher doping (overdoped). There are few materials in which this entire doping range can be accessed ($La_{2-x}Sr_xCuO_{4+\delta}$ is one), but this doping dependence of T_c is thought to be a generic feature of the hole-doped copper oxides. There are also materials that can be electron doped, but with a phase diagram in which the antiferromagnetic state persists to much higher doping, leaving a relatively narrow window of superconductivity[10].

The optimally doped regime on the hole-doped side has numerous properties at odds with Fermi-liquid theory, the standard theory of weakly interacting electrons that is the cornerstone of our understanding of metals. Most famously, the d.c. electrical resistivity has a linear temperature dependence[11] rather than the T^2 dependence expected for electrons scattering from one another. Signs of the magnetism persist far into this regime in the hole-doped materials, showing up as local order on short length scales observed in muon spin relaxation (μSR) measurements[12]. In neutron-scattering measurements, this local magnetic order appears as quartets of broadened, incommensurate peaks, with each quartet arranged around the $[\pm\pi/a, \pm\pi/a]$ Bragg peak position of the undoped antiferromagnet, but displaced by an amount that increases with hole doping[13–16]. Even when there is no longer static order, these peaks persist as excitations seen by inelastic neutron scattering. In the overdoped regime, on the right-hand side of the superconducting dome in Fig. 2, the copper oxides behave more like ordinary metals, showing a T^2 resistivity[17], for instance. This side of the phase diagram is best studied with $Tl_2Ba_2CuO_{6+\delta}$, a material that is naturally overdoped, not needing the substantial cation substitution required by $La_{2-x}Sr_xCuO_{4+\delta}$ to get into this regime. Not only are the transport properties more characteristic of a Fermi liquid, but T_c is low enough that readily accessible magnetic fields can drive the material normal (non-superconducting), enabling tests of Fermi-liquid theory down to low temperatures. $Tl_2Ba_2CuO_{6+\delta}$ has been shown to exhibit angular magnetoresistance oscillations that confirm the existence of a Fermi surface consistent with the predictions of conventional single-electron band theory[17,18]. The copper oxides manifest three major cornerstones of condensed-matter physics: a Fermi liquid described by single-electron theory, an insulator arising from a complete breakdown of single-electron theory, and a superconducting state perched in between these two archetypes. A desire for a global understanding of such disparate physics lies behind the enduring interest in the copper oxides because it demands that we take radically new approaches.

The biggest surprise in the story of the phase diagram was the discovery of another new ordered phase. When Nd was substituted for some of the La in $La_{2-x}Sr_xCuO_{4+\delta}$, a static charge-ordered phase was found[19]. A similar 'stripe' phase had already been seen in the $La_{2-x}Sr_xNiO_{4+\delta}$ system[20,21], an analogue of $La_{2-x}Sr_xCuO_{4+\delta}$. This phase consists of a stripe where

the doped holes mainly reside, separating regions of antiferromagnetic order for which the charge stripe provides an antiphase boundary for the magnetic order. The phase slip has a spacing that depends on the wavelength of the charge modulation, and thus provides an explanation for why the incommensurate peaks seen in neutron scattering are displaced from $[\pm\pi/a, \pm\pi/a]$ by an amount proportional to the hole doping. The stripe phase explains the tendency of T_c to be suppressed near a doping of 1/8 hole per Cu atom, where stripe periodicity becomes commensurate with the lattice spacing (shown as a depression in T_c near 1/8 doping in Fig. 2). This is prominent in $La_{1.6-x}Nd_xSr_{0.4}CuO_4$, in which the Nd substitution alters the tilt of the CuO_6 octahedra from an orthorhombic arrangement to a low-temperature tetragonal (LTT) phase, encouraging stripe order to rotate into an orientation parallel to the CuO_2 square-planar array and lock into static order[22]. The order 'melts' as doping is tuned away from 1/8 and without the Nd, the preferred orientation is diagonal to the square lattice. Similar evidence for ordered stripes is found in $La_{2-x}Ba_xCuO_{4+\delta}$, which possesses an LTT phase near 1/8 doping even without Nd (ref. 23). Recently the new technique of resonant X-ray scattering has led to a direct observation of the charge order in $La_{1.875}Ba_{0.125}CuO_4$, rather than inferring it from a combination of spin structure and lattice distortion[24]. In the past few years, many neutron-scattering measurements on different systems seem to converge on a common picture of the inelastic excitations. As energy is increased, the incommensurate peaks arrive at a strong resonance near 40 meV that becomes most apparent below the superconducting transition when the superconducting gap enhances the density of states at this energy. At higher energy the excitation spectrum disperses away from the antiferromagnetic wavevector $[\pm\pi/a, \pm\pi/a]$ (refs 25–27) in a manner reminiscent of the spin waves of the undoped system, but with an anisotropy that suggests that dynamic stripes might be playing a role. If magnetism is at the heart of the superconducting mechanism in the copper oxides, a detailed understanding of this magnetic excitation spectrum is crucial. There is now no doubt that stripe excitations occur in the cuprates and that statically ordered stripes suppress superconductivity. What is less clear, and thus a major topic of present research, is whether or not 'melted' stripes in a phase something like a nematic liquid crystal provide a good description of the underdoped cuprates and a mechanism for the superconductivity, or whether some more-conventional Fermi-liquid-based explanation can be used[28].

A NEW SUPERCONDUCTING PAIRING STATE

At the centre of this evolution from a Mott insulator to a relatively ordinary Fermi liquid lies the high-T_c superconducting phase. When confronted with a new superconductor, physicists ask if there is anything new about the state. Is this state different from the *s*-wave superconducting pairing state first formulated by Bardeen, Cooper and Schrieffer (BCS)[29,30] in 1957? 'Conventional' superconductors involve electrons paired into spin-singlet states that condense into a macroscopic wavefunction with the pairs strongly overlapping in real space. The pairs have no net momentum and no angular momentum, analogous to the $(s=0, l=0)$ *s*-shell of a hydrogen atom. BCS found this pairing state to arise when electrons near the Fermi surface of a degenerate Fermi gas have a weak attractive interaction, the standard source being interactions with phonons, the crystal lattice's normal modes of vibration. A number of these conventional features can be relaxed and still stay within the BCS framework, whose heart is the pairing of fermions and their condensation into the BCS wavefunction. An alternative type of condensation occurs in systems of bosons, where Bose statistics lead to condensation into a superfluid, the mechanism behind Bose–Einstein condensation in cold trapped atoms and in superfluid ^{4}He. Proof that the new superconductors involved pairing came by showing that magnetic flux trapped in cylinders was quantized in steps of $h/2e$, where h is Planck's constant, and $2e$ is the effective charge of the pairs that form the superconducting condensate[31], and by showing[32] that magnetic vortices in bulk samples were also quantized in units of $h/2e$. Direct imaging of these quantized bundles of magnetic flux provided a challenge for new scanning magnetic microscopy techniques. Scanning Hall microscopy[33] measurements were able to image individual vortices in bulk single crystals, and scanning SQUID microscopy[34] measured quantized flux trapped in micrometre-scale rings.

Staying within the BCS pairing framework, the most commonly considered deviation is pairing other than the spin-singlet, $l=0$ state. Such states were proposed in the 1960s[35,36], but a decade passed before the first experimental example, the superfluidity in ^{3}He, which involves spin-triplet pairing. Beyond this canonical example in a quantum fluid, the hunt for other exotic pairing states in solids has been an exasperating challenge. Several families of superconductors have presented

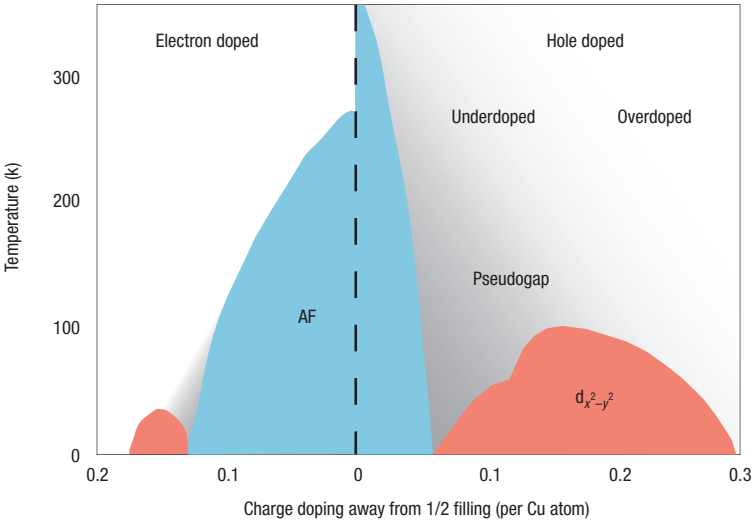

Figure 2 A schematic portrait of the copper oxide phase diagram. At half-filling (one unpaired electron per copper in the CuO_2 sheets) the cuprates are Mott insulators that order antiferromagnetically (AF). Holes can be doped into the planes by chemically altering other parts of the structure, rapidly suppressing the AF state and giving rise to a $d_{x^2-y^2}$ superconductor. The superconducting state evolves from the underdoped regime, where a large pseudogap in the density of states is seen in the 'normal state' (grey shaded region), to the overdoped regime in which the material is more like a normal metal. The planes can also be doped with electrons, giving rise to a rather different phase diagram with more robust antiferromagnetism and a small regime of superconductivity[10].

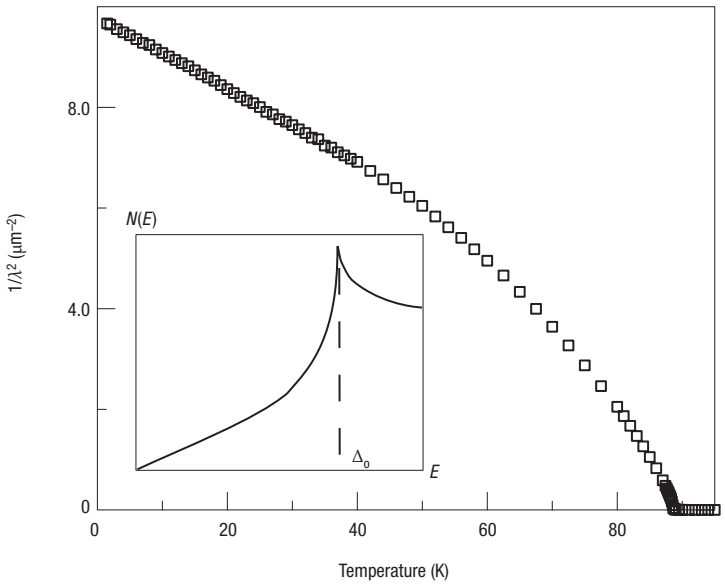

Figure 3 Measurement of the superfluid density derived from microwave measurements. The London penetration depth can be measured by determining the depth that microwave fields penetrate into the surface of a superconductor. The inverse square of this length scale is a measure of superfluid density, or phase stiffness, which sets a superconductor's resistance to variation in the phase of the superconducting wavefunction. The linear behaviour at low temperatures is a consequence of the linear density of states N on energy E (inset) of a $d_{x^2-y^2}$ superconductor with a cylindrical Fermi surface. The energy gap Δ of this state has a maximum Δ_0 for momenta in the direction of the Cu–O bonds, but nodes in the diagonal directions that give rise to the linear density of states at low energy.

candidates: the organic superconductors, heavy-fermion superconductors and most recently strontium ruthenate. The primary issue that makes this quest difficult is sample quality. The *s*-wave, spin-singlet superconductors are in a very special state of matter, protected from the influence of defects by Anderson's theorem[37]. They possess an energy gap in their excitation spectrum that is little affected by non-magnetic impurities because it breaks no symmetries of the materials' crystal structure. Non-*s*-wave superconductors break additional symmetries, possess energy gaps that change sign on reflection or rotation, and also possess nodes on the Fermi surface. When the sign of the superconducting wavefunction can change through a scattering event, impurities become highly disruptive, masking many of the low-temperature properties, or even killing superconductivity entirely.

The cuprates offer one of the great successes in the identification of a new pairing state[6]. First, NMR measurements of the Knight shift showed that the spin susceptibility falls rapidly below T_c, proof that the superconducting pairs are not in a spin-triplet state[38,39]. This requires the orbital part of the pairing wavefunction to be symmetric, either the $l = 0$ *s*-wave state or some higher angular momentum such as $l = 2$ (*d*-wave). In 1993, microwave measurements of the temperature dependence of the London penetration depth, λ, showed linear temperature dependence consistent with a *d*-wave density of states[40]. Figure 3 shows $1/\lambda^2$, referred to as the superfluid density, in analogy to the two-fluid model of superfluid ^{4}He. More correctly, it is not a density but a tensor quantity known as phase stiffness that determines a superconductor's resistance to variation in the phase of the superconducting order parameter. As the temperature increases, quasiparticle excitations deplete the superfluid density until it falls to zero when the normal state is reached. A *d*-wave state would possess lines of nodes on the cylindrical Fermi surface expected for these layered materials, and there would thus be quasiparticle excitations possible down to zero energy, with a density of states varying linearly with energy. The linear temperature dependence of $1/\lambda^2(T)$ was masked by impurities in earlier measurements, something subsequently confirmed when it was shown that substituting Zn impurities on the Cu site could change the low-temperature power laws[41–43]. It took six years for the field to produce samples of sufficient quality to find the *d*-wave superconducting state — nature had given us a delicate pairing state wrapped in a very difficult materials problem. The drive to uncover the intrinsic behaviour of these materials has led to the development of materials up to 99.999% pure, and with high crystalline perfection[44,45]. Although not at the level that has been achieved over decades of semiconductor development, this level of control is exceptional in transition metal oxides.

Further identification came from experimental techniques far beyond those used in the era of BCS. One of these is angle-resolved photoemission spectroscopy (ARPES), which uses the photoelectric effect to map the energy and momentum of filled states near the Fermi energy[46]. The technique is particularly suited to quasi-two-dimensional materials, and had an energy resolution in the early 1990s that was close to that necessary to see the superconducting energy gap of the copper oxides. The extraordinary development of ARPES was fuelled by the prize of observing the variation of an unconventional energy gap around a Fermi surface, a quest that led to an improvement in resolution by more than an order of magnitude in less than a decade. The material for the job was $Bi_2Sr_2CaCu_2O_{8+\delta}$, which possesses a cleavage plane between two weakly van der Waals-bound BiO layers, providing an ideal surface for spectroscopy, with no surface states or reconstruction. The energy gap mapped out by ARPES near the Fermi energy (Fig. 4) was indeed consistent with nodes in the gap function, which ARPES showed lay in the [110] direction, rotated 45° from the orientation of the square CuO_2 lattice[47,48] — a possible $d_{x^2-y^2}$ state.

The finish to the identification of the new state was an ingenious experiment that directly observed the extra broken symmetry. A film was grown on a tricrystal substrate, one where the three crystal orientations of the fused substrate frustrated the orientation of the $d_{x^2-y^2}$ state[49]. In trying to follow the orientation of the substrate lattice, the $d_{x^2-y^2}$ state finds itself changing sign on rotation through 360° about the axis at which the three orientations met. A superconducting ring patterned around this axis solves the frustration by spontaneously running a supercurrent that sustains half of a superconducting

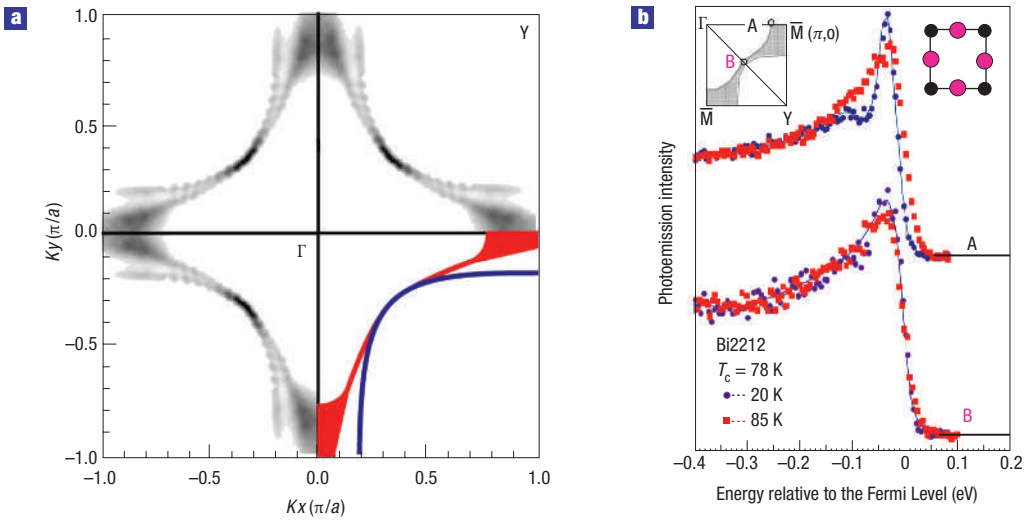

Figure 4 ARPES measurements of the Fermi surface and anisotropic superconducting gap. **a**, A recent ARPES determination of the Fermi surface of $Bi_2Sr_2CaCu_2O_{8+\delta}$ (Bi2212), the surface in momentum space (*Kx*, *Ky*) that marks the boundary between filled and empty states. Recent improvements in resolution now show that the Fermi surface consists of two concentric hole-like cylinders because the unit cell of this crystal structure contains a pair of CuO_2 sheets[94]. **b**, The difference in the size of the superconducting gap at two different locations A and B on the Fermi surface. In the Γ-M direction (Cu–O bond direction) a large gap in the density of states opens at the Fermi surface, but in the Γ-Y direction 45 degrees away from this, no gap is seen. Part **b** reprinted with permission from ref. 47. Copyright (1993) by the American Physical Society.

flux quantum (1/2 of $h/2e$), a crisp yes–no result observed by integrating the flux in an image obtained with a scanning SQUID microscope[49]. In one fell swoop, the pairing state was nailed down, a new scanning microscopy technique for imaging fields proved its mettle, and a rather exotic superconducting device structure had been fabricated in a thin film. The tricrystal experiment has confirmed the $d_{x^2-y^2}$ pairing state in the main families of copper oxide superconductors over a wide range of doping[50], including the electron-doped ones[51]. The sign change of the $d_{x^2-y^2}$ state on rotation through 90° leads to related effects in experiments involving tunnelling into an *s*-wave state. A corner junction in which an *s*-wave superconductor connects to both signs of the $d_{x^2-y^2}$ wavefunction found at neighbouring edges on a 90° corner gives rise to a minimum in the critical current of the junction in zero magnetic field, rather than the peak seen for an *s*-wave to *s*-wave junction[52]. Figure 5 shows a more recent design using ramp junctions between $YBa_2Cu_3O_{6+x}$ and Nb that has enabled large numbers of these structures to be fabricated, moving this area into the realm of actual devices and applications[53]. The advantage is that the phase of the $d_{x^2-y^2}$ state is actually useful, leading to simplifications in SQUID electronics and a potential flux qubit, one that doesn't need to be biased with a magnetic field[54].

Over the past decade the $d_{x^2-y^2}$ pairing state has come under intense scrutiny — not just the new pairing symmetry, but also the framework of BCS theory[17]. Noteworthy successes include the measurement of a universal limit as $T \rightarrow 0$ in thermal conductivity[55], the dependence of that thermal conductivity on magnetic field[56] and the cusp-like microwave conductivity spectra seen in $YBa_2Cu_3O_{6.50}$[57]. These tests depended on the development of high-purity $YBa_2Cu_3O_{6+x}$ crystals with mean free paths on the micrometre scale, something extraordinary in a quaternary compound[45]. The effects of impurities and vortices have been probed in a very new way with scanning tunnelling spectroscopy (STS). Before the advent of this technique, the influence of impurities could only be inferred from bulk properties, but STS brings the ability to measure electronic spectra locally with atomic resolution. For instance, spatially resolved images of the density of states in the vicinity of impurity atoms such as Ni and Zn on the Cu sites in the CuO_2 planes confirm the impact of such impurities on the $d_{x^2-y^2}$ density of states[58,59] and provide information that can be folded into calculations of the bulk properties. The basic story at the present time is that for optimal and overdoped samples, a treatment of nodal quasiparticles within a relatively conventional BCS framework accounts for many of the low-energy and low-temperature properties of the copper oxides. In the underdoped regime this picture runs into its greatest difficulties.

FLUCTUATING SUPERCONDUCTIVITY

A surprise offered by the copper oxide materials is the large role played by fluctuations of the superconducting order parameter. A superconducting transition is usually second order, and for most superconductors this transition is well described by BCS theory, a mean-field theory in which the order parameter is uniformly suppressed to zero as T_c is approached. Fluctuations are not seen because the coherence length is typically large,

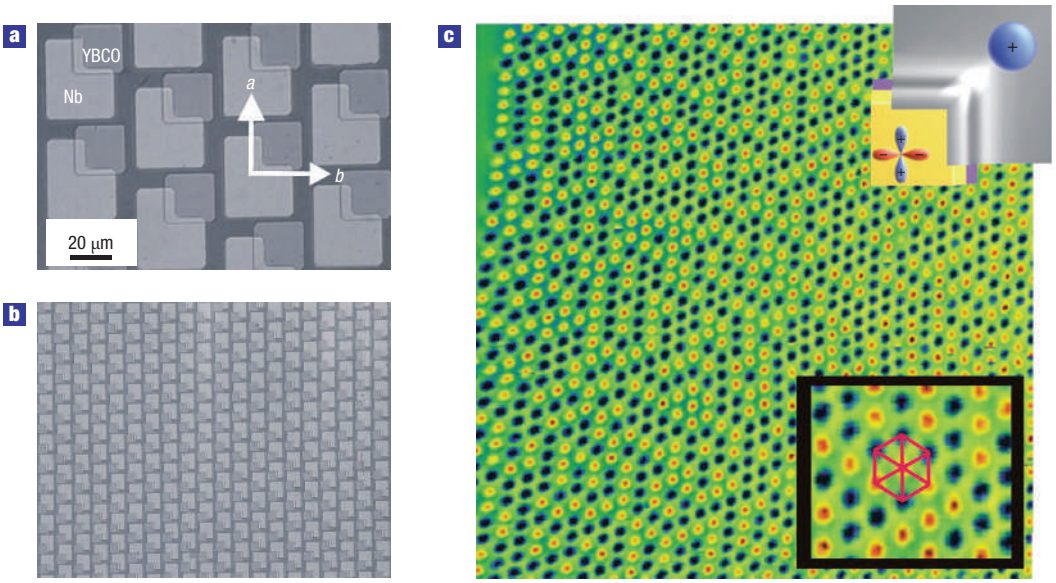

Figure 5 Half-flux quanta in an array of ramp junctions. **a**,**b**, A closeup view of corner junctions between Nb and squares of $YBa_2Cu_3O_{6+x}$ (**a**). The junctions use a new ramp-junction geometry that enables highly reproducible, lithographically-defined structures as shown in the expanded view in panel (**b**). **c**, A scanning SQUID image of the array of half-flux quanta spontaneously generated by this array of junctions. The half-flux quanta are spontaneously generated in order to resolve the problem that the *s*-wave state in Nb must connect opposite signs of the wavefunction of the $d_{x^2-y^2}$ state of $YBa_2Cu_3O_{6+x}$ (ref. 53).

making it too costly to create fluctuating patches of normal material in the superconducting state or superconductor in the normal state. In the copper oxides, the high T_c carries a correspondingly large energy gap, and a short coherence length of a nanometre or two. This makes fluctuations much more important and such effects are further promoted by the extreme anisotropy of these layered materials[60,61]. A third factor that enhances the role of fluctuations is the anomalously low phase stiffness, particularly on the underdoped side of the phase diagram. Samples at optimal doping have phase stiffness an order of magnitude smaller than most metallic superconducting compounds and elements, owing to the low carrier density in these oxides. As doping is decreased, μSR has shown[62] the phase stiffness falling lower with T_c.

All of these features, low phase stiffness, short coherence length and layered structure give rise to prominent fluctuation effects near T_c. The phase stiffness itself is a clean example, with the behaviour shown in Fig. 3 governed by a power law near T_c that is close to the critical exponent $\nu = 0.33$ expected for 3DXY critical fluctuations[63]. 3DXY is the universality class for a neutral three-dimensional superfluid governed by a two-component order parameter, namely the magnitude and phase of the superconducting order parameter. The fact that it is a charged superfluid is not expected to manifest itself until much closer to T_c, so for the measurable temperature range near T_c, the universal exponents of the copper oxides are the same as those of superfluid ^{4}He. The power of critical fluctuations is that once the universality class is known, many properties can be predicted from scaling theories, without detailed microscopic models. For instance, the well-known lambda-shaped anomaly in the specific heat of superfluid ^{4}He should also appear in the copper oxides' specific heat. This has been difficult to discern because there is a dominant lattice contribution to the specific heat, though specific-heat measurements in magnetic field favour 3DXY scaling[64]. Thermal expansion is a related measurement with the advantage that in $YBa_2Cu_3O_{6+x}$, taking the difference between the *a* and *b* axis thermal expansion cancels out most of the lattice background[65]. Figure 6 shows the progression of the thermal expansion anomaly as a function of hole-doping in $YBa_2Cu_3O_{6+x}$. At the highest hole-doping, the transition looks more like the jump expected for a mean-field transition, rounded by fluctuations, but at lower doping the curves evolve into the cusps expected for an anisotropic 3DXY transition, with fluctuations persisting over a wide temperature range above and below T_c (ref. 66).

The survival of superconducting fluctuations far above T_c in the underdoped copper oxides has been observed by terahertz spectroscopy[67] and high-resolution magnetic susceptibility measurements[68]. When a magnetic field is applied, fluctuations are also found in the Nernst effect[69,70]. In this measurement, a thermal gradient produces a voltage perpendicular to both the applied magnetic field and the temperature gradient, and the large size of this effect in the copper oxides suggests that magnetic vortices persist far above T_c and generate a transverse voltage as they drift in response to the thermal gradient. This dominant role of fluctuations requires a major shift in how one thinks about the phase diagram. If critical fluctuations govern the transition in zero field, then they also drastically affect the behaviour in a magnetic field. In

conventional superconductors, mean-field theory is used to give a description of the superconducting state in the presence of a magnetic field. This treatment leads to a phase diagram characterized by two critical fields. Below H_{c1}, the superconductor is in the Meissner state and completely excludes fields from the bulk of the sample; between H_{c1} and H_{c2} there is a vortex state, where quantized magnetic vortices thread through the sample and typically form a triangular lattice, a vortex solid; above H_{c2} the sample is in its normal state. In a theory that includes critical fluctuations, H_{c2} becomes a crossover rather than a phase transition and the true phase transitions in increasing field are H_{c1}, followed by a vortex lattice melting transition[61]. The first-order vortex melting transition has been observed as a peak in critical current due to a loss of shear modulus just below the transition[71], a peak in magnetic damping in a torsional oscillator[72], a step in magnetization[73], and measurements of hysteretic steps in the electrical resistivity[74].

The effect of fluctuations on the phase diagram has practical as well as fundamental consequences. In a vortex solid state, the vortex lattice is pinned to defects and the superconductor can still carry current without resistance, the basis for any high-current application of a superconductor. Learning how to pin vortices was the key behind the development of superconducting wire now used in high-field magnets such as those in magnetic resonance imaging machines. The promise of high-power applications of the high-temperature superconductors depends on a similar control over vortex motion, but the task is made harder by the presence of thermal fluctuations. In the vortex state at relatively high temperatures, the lattice can melt so that vortices are no longer well-pinned by defects, resulting in a loss of zero resistance. Even worse, extreme anisotropy means that vortices act more like a weakly correlated stack of vortex 'pancakes' rather than a line, making them even harder to pin[75]. With these fundamental difficulties recognized, work towards practical applications has forged ahead, especially in niche power applications such as leads for superconducting magnets and devices for improving power quality[76]. Alongside this practical effort, the vortex state in the copper oxides has been a driving force in the study of vortex matter[77], which uses these materials as a medium in which to study the individual and collective behaviour of vortices.

As for the core problem of understanding the copper oxides themselves, the remaining debate over fluctuations and critical behaviour lies in quantifying how big a role they play in the anomalous properties of these materials. The evidence outlined above shows that in zero field, superconducting fluctuations extend far into the 'normal' state, that critical fluctuations can be observed, and that a vortex liquid state persists over a wide range of temperatures and magnetic fields. A further step beyond this suggests that the key features of the underdoped side of the phase diagram are controlled by very strong pairing that is phase-disordered by fluctuations. This scenario was initially driven by the correlation between T_c and phase stiffness as

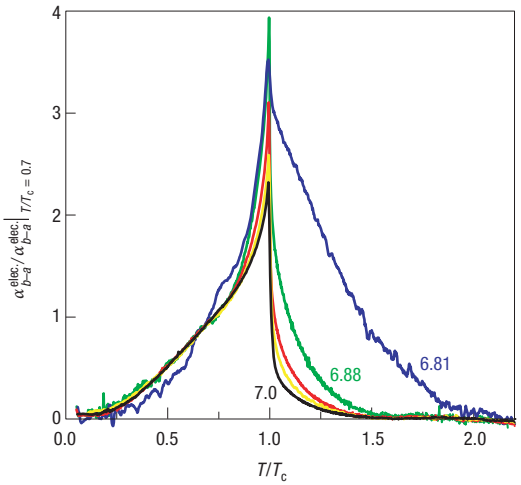

Figure 6 Superconducting fluctuations in thermal expansion. The thermal expansion of $YBa_2Cu_3O_{6+x}$ has a cusp-shaped anomaly at T_c due to fluctuations of the superconducting order parameter. As the doping is decreased, the fluctuations rapidly extend to temperatures far above T_c. Reprinted with permission from ref. 66. Copyright (2001) by the American Physical Society.

hole-doping is changed in the underdoped regime[62], the argument being that T_c is controlled by the phase stiffness, not the strength of the pairing on the underdoped side of the phase diagram[78–80]. This is different from BCS theory, in which superconductivity disappears with increasing temperature because the superconducting order parameter $|\Delta|e^{i\Phi}$ has its magnitude $|\Delta|$ driven to zero at T_c. The alternative is that T_c is set by the disordering of the phase Φ because the phase stiffness is so low. The other aspect of the phase diagram that supports this scenario is the presence of a large 'pseudogap' in the underdoped copper oxides, over a wide temperature range in which there are numerous spectroscopic indications that a partially formed energy gap opens up in the density of states[81], indicated as a shaded area in the phase diagram in Fig. 2. This suggests that the gap marks the onset of pairing at rather high temperatures, but that T_c is set by the onset of phase coherence at lower temperatures — much lower when T_c and the phase stiffness are driven down by decreasing the hole doping. An alternative view is that the pseudogap is the result of some competing ordered phase, but evidence for an actual phase transition to a competing phase has remained elusive and controversial. The fact that the pseudogap behaviour becomes increasingly apparent as doping approaches the antiferromagnetic insulator also suggests that the underdoped regime is influenced by Mott physics, where the strong interactions lead to an insulator at half-filling.

Fluctuations and critical behaviour have also been invoked to explain the strange electronic properties of the copper oxides, in terms of quantum critical points (QCPs). Numerous measurements in the normal state show an evolution from the pseudogap phase at low doping to a high doping

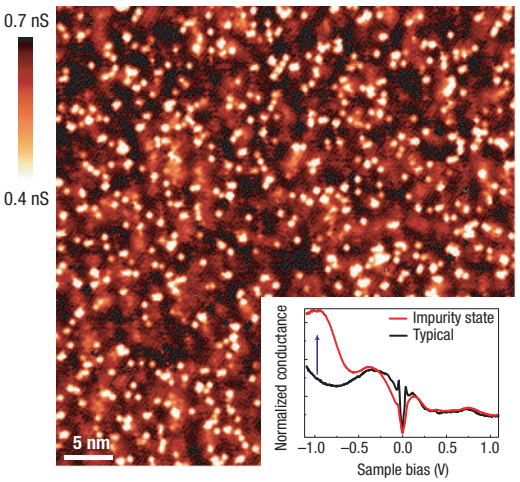

Figure 7 STS measurements on $Bi_2Sr_2CaCu_2O_{8+\delta}$. The image is a scan of the surface at a bias voltage of −0.9 V where an impurity state appears in the tunnelling spectrum, as indicated by the arrow in the inset. Variation of doping and the energy of the impurity state suggest that this is the interstitial O^{2-} ion that controls the hole doping in this material. The location of these impurities is strongly correlated with a spatially inhomogeneous spectrum. Regions far from an impurity display a conventional $d_{x^2-y^2}$ spectrum with sharp peaks at the gap maximum Δ_0. Near the defects, the sharp peaks are washed out and the gap appears larger. Reprinted with permission from ref. 90. Copyright 2005 AAAS.

range for which Fermi-liquid theory provides a good starting point. In between, around optimal doping, the materials show some of their most anomalous properties, such as the d.c. resistivity being linear over a very wide temperature range[11]. This range seems governed by no energy scale other than temperature, something associated with quantum criticality. The suggestion is that a QCP lies at $T = 0$, obscured under the superconducting dome[82], and that these anomalous properties, and even the superconductivity itself, arise from it. The behaviour of the d.c. resistivity in high magnetic field provides one of many clues to this evolution, showing that the low-temperature resistivity when superconductivity is suppressed seems to be insulating on the underdoped side of the phase diagram and metallic on the overdoped side[83].

DISORDER, NEW METHODS, NEW MATERIALS

The advances described above — identifying a new superconducting state, the importance of fluctuations and the importance of strong correlations and magnetism — are all affected by the major challenge of understanding and controlling the effects of defects and inhomogeneity. Many of the properties discovered thus far point to a high degree of intrinsic sensitivity to disorder of all kinds: the *d*-wave superconducting state is more sensitive to disorder than other pairing states; the antiferromagnet is disturbed by hole doping; charge-ordered states lie nearby and depend on details of chemical composition and structure. Short coherence lengths, low phase stiffness and extreme anisotropy make it easy to have superconducting samples that are spatially inhomogeneous or even fluctuating and completely phase disordered.

One highly controllable way to see the intrinsic sensitivity of these materials is to apply a large magnetic field, driving the material into a vortex state in which the cores of the vortices are normal and a large magnetic field is distributed through the bulk of the sample. Neutron-scattering measurements in magnetic field show an enhanced signal at the incommensurate peaks near $[\pm\pi/a, \pm\pi/a]$, suggesting that the entire sample becomes more magnetic[84,85]. μSR measurements in $YBa_2Cu_3O_{6+x}$ have also suggested that the vortex cores are antiferromagnetic[86]. A local, real-space view of this sensitivity has come from new developments in STS. In the vortex state, the cores should have an electronic spectrum different from the surrounding *d*-wave superconducting state. Outside the core, the density of states should possess the gap structure of a *d*-wave superconductor, so by scanning at an energy where this differs from the core spectra, the cores can be imaged. This was applied to $YBa_2Cu_3O_{6+x}$ to image the vortex lattice and the elliptical shape of the vortex cores caused by in-plane anisotropy in this orthorhombic material[87]. The technique has reached extraordinary detail in $Bi_2Sr_2CaCu_2O_{8+\delta}$. By taking the difference between STS images in field and in zero field, high-resolution spectroscopy of the vortex state revealed a checkerboard pattern of charge-density modulation in the vortex cores[88]. A similar checkerboard pattern has now been seen in the normal state on the surface of lightly doped $Ca_{2-x}Na_xCuO_2Cl_2$, a related copper oxide[89].

$Bi_2Sr_2CaCu_2O_{8+\delta}$ also seems to be dominated by substantial inhomogeneity on the mesoscale even in zero field. Point-by-point spectroscopic measurements across a field of view show the magnitude of the gap, varying from regions with a nearly ideal-looking density of states for a *d*-wave superconductor to other patches with a larger gap and suppressed peaks at the gap edge. Most recently, this inhomogeneity in the gap has been found to correlate with the location of interstitial oxygen dopant atoms[90], as illustrated in Fig. 7. This discovery should stimulate questions and concerns about the impact dopant atoms have on the physics of the copper oxides. The model material La_2CuO_4 is a stoichimetric compound in its undoped antiferromagnetic state, and is most commonly doped by substitution of Sr or Ba on the La site, a cation defect lying in the layer immediately adjacent to the CuO_2 planes. By comparison, the interstitial oxygen used to control the doping of $Bi_2Sr_2CaCu_2O_{8+\delta}$ is a gentler perturbation, separated from the CuO_2 layers by an intervening SrO layer, yet causing substantial electronic inhomogeneity. This is manifest in other properties such as a large residual density of carriers that never condense into the superfluid[91]. In $YBa_2Cu_3O_{6+x}$, the doping comes from a layer of CuO_x chains separated from the CuO_2 planes by a BaO layer. The unusual feature of the doping in $YBa_2Cu_3O_{6+x}$ is that the oxygen in these chains is rather loosely bound, easily removed

or replaced by annealing at moderate temperatures. They are also still mobile within the sample even at room temperature, and can be ordered into a number of crystalline phases. Thus, in this system, doping is not necessarily associated with chemical disorder. $YBa_2Cu_3O_6$, an insulating antiferromagnet with no dopant oxygens, is a stoichiometric compound, but so is $YBa_2Cu_3O_7$ with almost perfectly filled CuO chains[92]. $YBa_2Cu_3O_{6.50}$ carefully prepared has every other chain filled with oxygen. There is also a perfectly ordered stoichiometric compound with a double chain layer that gives an underdoped material with a T_c of 85 K. These compounds can be prepared with exceptional purity and crystalline perfection because they do not suffer from cation non-stoichiometry, as happens for instance in $Bi_2Sr_2CaCu_2O_{8+\delta}$, which is often closer to a composition of $Bi_{2.2}Sr_{1.8}CaCu_2O_{8+\delta}$, or $Tl_2Ba_2CuO_{6+\delta}$, which is usually closer to $Tl_{1.9}Ba_2Cu_{1.1}O_{6+\delta}$. Manipulating such cation non-stoichiometry has been shown[93] to have a substantial impact on T_c. One consequence of the perfection of the highly ordered $YBa_2Cu_3O_{6+x}$ phases is that the quasiparticle excitations in the superconducting state develop transport mean free paths on a micrometre scale[57]. Unfortunately, $YBa_2Cu_3O_{6+x}$ does not possess a suitable cleavage plane for STS or ARPES measurements, so these important techniques are for the moment focused on compounds with more suitable cleavage planes, $Bi_2Sr_2CaCu_2O_{8+\delta}$ being the ideal example. This leaves the field in a materials conundrum in which some of the most powerful techniques developed during the pursuit of the high-temperature superconductivity problem are not easily used on the cleanest samples we have available to us. Getting past this problem may require new materials, as well as further breakthroughs in experimental techniques.

CONCLUSIONS

High-temperature superconductors are remarkably different from the superconducting elements and intermetallic compounds and alloys — different in more ways than anyone anticipated in 1986–87. The copper oxides exhibit at least two new states of matter, $d_{x^2-y^2}$ superconductivity and charge stripes, embedded in a contest between two very different paradigms of condensed-matter physics — the theory of weakly interacting electrons in a crystalline lattice pitted against strongly correlated electrons and Mott physics. The enduring goal is to achieve a more-unified understanding of all these phenomena. Enormous progress has been made on different aspects of this problem, yielding new theoretical ideas and computational techniques that have wide applicability as we move beyond traditional metals, semiconductors and insulators. On the technological front, new experimental techniques such as STS, scanning magnetic microscopy and ARPES have all cut their teeth on the copper oxides. The new pairing state, the anomalously low phase stiffness, short coherence length and prominence of fluctuations have also had an impact on our approach to applications of high-temperature superconductors. These properties placed obstacles in the path of high-power applications such as long-distance power transmission and levitating trains, but understanding those problems has meant progress on applications for wire able to carry high current densities with low or zero resistance. What was not anticipated in 1986 is that a proper understanding of the d-wave superconducting state would lead to unforeseen possibilities in electronics and wireless applications. The d-wave pairing state, despite all of its delicacy, also has unique features in the phase of the superconducting wavefunction that create new opportunities in electronics.

doi:10.1038/nphys248

References

1. Bednorz, J. G. & Müller, K. A. Possible high T_c superconductivity in the Ba-La-Cu-O system. *Z. Phys. B* **64,** 189–193 (1986).
2. Wu, M. K. *et al.* Superconductivity at 93 K in a new mixed-phase Yb-Ba-Cu-O compound system at ambient pressure. *Phys. Rev. Lett.* **58,** 908–910 (1987).
3. Sun, G. F., Wong, K. W., Xu, B. R., Xin, Y. & Lu, D. F. T_c enhancement of $HgBa_2Ca_2Cu_3O_{8+\delta}$ by Tl substitution. *Phys. Lett. A* **192,** 122–124 (1994).
4. Sleight, A. W., Gillson, J. L. & Bierstedt, P. E. High-temperature superconductivity in the $BaPb_{1-x}Bi_xO_3$ systems. *Solid State Commun.* **17,** 27–28 (1975).
5. Scalapino, D. J., Loh, E. & Hirsch, J. E. d-wave pairing near a spin-density-wave instability. *Phys. Rev. B* **34,** 8190–8192 (1986).
6. Scalapino, D. J. The case for $d_{x^2-y^2}$ pairing in the cuprate superconductors. *Phys. Rep.* **250,** 329–365 (1995).
7. Anderson, P. W. The resonating valence bond state in La_2CuO_4 and superconductivity. *Science* **235,** 1196–1198 (1987).
8. Vaknin, D. *et al.* Antiferromagnetism in La_2CuO_{4-y}. *Phys. Rev. Lett.* **58,** 2802–2805 (1987).
9. Tranquada, J. M. *et al.* Neutron-diffraction determination of antiferromagnetic structure of Cu ions in $YBa_2Cu_3O_{6+x}$ with $x = 0.0$ and 0.15. *Phys. Rev. Lett.* **60,** 156–159 (1988).
10. Alff, L. *et al.* A hidden pseudogap under the 'dome' of superconductivity in electron-doped high-temperature superconductors. *Nature* **422,** 698–701 (2003).
11. Batlogg, B. *et al.* Normal state phase diagram of $(La, Sr)_2CuO_4$ from charge and spin dynamics. *Physica C* **235,** 130–133 (1994).
12. Niedermayer, C. *et al.* Common phase diagram for antiferromagnetism in $La_{2-x}Sr_xCuO_4$ and $Y_{1-x}Ca_xBa_2Cu_3O_6$ as seen by muon spin rotation. *Phys. Rev. Lett.* **80,** 3843–3846 (1998).
13. Thurston, T. R. *et al.* Neutron scattering study of the magnetic excitations in metallic and superconducting $La_{2-x}Sr_xCuO_{4-y}$. *Phys. Rev. B* **40,** 4585–4595 (1989).
14. Cheong, S.-W. *et al.* Incommensurate magnetic fluctuations in $La_{2-x}Sr_xCuO_4$. *Phys. Rev. Lett.* **67,** 1791–1794 (1991).
15. Mason, T. E., Aeppli, G. & Mook, H. A. Magnetic dynamics of superconducting $La_{1.86}Sr_{0.14}CuO_4$. *Phys. Rev. Lett.* **68,** 1414–1417 (1992).
16. Thurston, T. R. *et al.* Low-energy incommensurate spin excitations in superconducting $La_{1.85}Sr_{0.15}CuO_4$. *Phys. Rev. B* **46,** 9128–9131 (1992).
17. Hussey, N. Low-energy quasiparticles in high-T_c cuprates. *Adv. Phys.* **51,** 1685–1771 (2002).
18. Hussey, N., Abdel-Jawad, M., Carrington, A., Mackenzie, A. & Balicas, L. A coherent three-dimensional fermi surface in a high-transition-temperature superconductor. *Nature* **425,** 814–817 (2003).
19. Tranquada, J. M., Sternlieb, B. J., Axe, J. D., Nakamura, Y. & Uchida, S. Evidence for stripe correlations of spins and holes in copper oxide superconductors. *Nature* **375,** 561–563 (1995).
20. Tranquada, J. M., Buttrey, D. J., Sachan, V. & Lorenzo, J. E. Simultaneous ordering of holes and spins in $La_2NiO_{4.125}$. *Phys. Rev. Lett.* **73,** 1003–1006 (1995).
21. Sachan, V., Buttrey, D. J., Tranquada, J. M., Lorenzo, J. E. & Shirane, G. Charge and spin ordering in $La_{2-x}Sr_xNiO_{4.00}$ with $x = 0.135$ and 0.20. *Phys. Rev. B* **51,** 12742–12746 (1995).
22. Tranquada, J. M. *et al.* Coexistence of, and competition between, superconductivity and charge-stripe order in $La_{1.6-x}Nd_{0.4}Sr_xCuO_4$. *Phys. Rev. Lett.* **78,** 338–341 (1997).
23. Fujita, M., Goka, H., Yamada, K., Tranquada, J. M. & Regnault, L. P. Stripe order, depinning, and fluctuations in $La_{1.875}Ba_{0.125}CuO_4$ and $La_{1.875}Ba_{0.075}Sr_{0.050}CuO_4$. *Phys. Rev. B* **70,** 104517 (2004).
24. Abbamonte, P. *et al.* Spatially modulated 'mottness' in $La_{2-x}Ba_xCuO_4$. *Nature Phys.* **1,** 155–158 (2005).
25. Hayden, S. M., Mook, H. A., Dai, P., Perring, T. G. & Doan, F. The structure of the high-energy spin excitations in a high-transition temperature superconductor. *Nature* **429,** 531–534 (2004).
26. Hinkov, V. *et al.* Two-dimensional geometry of spin excitations in the high-transition-temperature superconductor $YBa_2Cu_3O_{6+x}$. *Nature* **430,** 650–654 (2004).
27. Tranquada, J. M. *et al.* Quantum magnetic excitations from stripes in copper oxide superconductors. *Nature* **430,** 534–538 (2004).
28. Kivelson, S. A. *et al.* How to detect fluctuating stripes in the high-temperature superconductors. *Rev. Mod. Phys.* **75,** 1201–1241 (2003).
29. Bardeen, J., Cooper, L. N. & Schrieffer, J. R. Microscopic theory of superconductivity. *Phys. Rev.* **106,** 162–164 (1957).

30. Bardeen, J., Cooper, L. N. & Schrieffer, J. R. Theory of superconductivity. *Phys. Rev.* **108,** 1175–1204 (1957).
31. Gough, C. E. *et al.* Flux quantization in a high-T_c superconductor. *Nature* **326,** 855 (1987).
32. Gammel, P. L. *et al.* Observation of hexagonally correlated flux quanta in $YBa_2Cu_3O_7$. *Phys. Rev. Lett.* **59,** 2592–2595 (1996).
33. Wynn, J. C. *et al.* Limits on spin-charge separation from $h/2e$ fluxoids in very underdoped $YBa_2Cu_3O_{6+x}$. *Phys. Rev. Lett.* **87,** 197002 (2001).
34. Bonn, D. A. *et al.* A limit on spin-charge separation in high-T_c superconductors from the absence of a vortex-memory effect. *Nature* **414,** 887–889 (2001).
35. Anderson, P. W. & Morel, P. Generalized Bardeen-Cooper-Schrieffer states and the proposed low-temperature phase of liquid He^3. *Phys. Rev.* **123,** 1911–1934 (1961).
36. Balian, R. & Werthamer, N. R. Superconductivity with pairs in a relative p wave. *Phys. Rev.* **131,** 1553–1564 (1963).
37. Anderson, P. W. Knight shift in superconductors. *Phys. Rev. Lett.* **3,** 325–326 (1959).
38. Takigawa, M., Hammel, P. C., Heffner, R. H. & Fisk, Z. Spin susceptibility in superconducting $YBa_2Cu_3O_7$ from ^{63}Cu Knight shift. *Phys. Rev. B* **39,** 7371–7374 (1989).
39. Barrett, S. E. *et al.* ^{63}Cu Knight shifts in the superconducting state of $YBa_2Cu_3O_{7-\delta}$ ($T_c = 90$ K). *Phys. Rev. B* **41,** 6283–6296 (1990).
40. Hardy, W. N., Bonn, D. A., Morgan, D. C., Liang, R. & Zhang, K. Precision measurements of the temperature dependence of lambda in $YBa_2Cu_3O_{6.95}$: Strong evidence for nodes in the gap function. *Phys. Rev. Lett.* **70,** 3999–4002 (1993).
41. Achkir, D., Poirier, M., Bonn, D. A., Liang, R. & Hardy, W. N. Temperature dependence of the in-plane penetration depth of $YBa_2Cu_3O_{6.95}$ and $YBa_2(Cu_{0.9985}Zn_{0.0015})_3O_{6.95}$ crystals from T to T^2. *Phys. Rev. B* **48,** 13184–13187 (1993).
42. Bonn, D. A. *et al.* Comparison of the influence of Ni and Zn impurities on the electromagnetic properties of $YBa_2Cu_3O_{6.95}$. *Phys. Rev. B* **50,** 4051–4063 (1994).
43. Kitaoka, Y. Cu NMR and NQR studies of impurities-doped $YBa_2(Cu_{1-x}M_x)_3O_7$ (M = Zn and Ni). *J. Phys. Soc. Jpn* **62,** 2803–2818 (1993).
44. Erb, A., Walker, E. & Flukiger, R. $BaZrO_3$: the solution to the crucible corrosion problem during the single crystal growth of high-T_c superconductors; $REBa_2Cu_3O_{7-\delta}$ RE = Y, PR. *Physica C* **245,** 245–251 (1995).
45. Liang, R., Bonn, D. A. & Hardy, W. N. Growth of high quality YBCO single crystals using $BaZrO_3$ crucibles. *Physica C* **304,** 105–111 (1998).
46. Damascelli, A., Hussain, Z. & Shen, Z.-X. Angle-resolved photoemission studies of the cuprate superconductors. *Rev. Mod. Phys.* **75,** 473–541 (1994).
47. Shen, Z.-X. *et al.* Anomalously large gap anisotropy in the a-b plane of $Bi_2Sr_2CaCu_2O_{8+\delta}$. *Phys. Rev. Lett.* **70,** 1553–1556 (1993).
48. Ding, H. *et al.* Angle-resolved photoemission spectroscopy study of the superconducting gap anisotropy in $Bi_2Sr_2CaCu_2O_{8+x}$. *Phys. Rev. B* **54,** 9678–9681 (1996).
49. Tsuei, C. C. *et al.* Pairing symmetry and flux quantization in a tricrystal superconducting ring of $YBa_2Cu_3O_{7-\delta}$. *Phys. Rev. Lett.* **73,** 593–596 (1994).
50. Tsuei, C. C. *et al.* Robust $d_{x^2-y^2}$ pairing symmetry in hole-doped cuprate superconductors. *Phys. Rev. Lett.* **93,** 187004 (2004).
51. Tsuei, C. C. & Kirtley, J. R. Phase-sensitive evidence for d-wave pairing symmetry in electron-doped cuprate superconductors. *Phys. Rev. Lett.* **85,** 182–185 (2000).
52. Wollman, D. A., Harlingen, D. J. V., Lee, W. C., Ginsberg, D. M. & Leggett, A. J. Experimental determination of the superconducting pairing state in YBCO from the phase coherence of YBCO-Pb dc SQUIDs. *Phys. Rev. Lett.* **71,** 2134–2137 (1993).
53. Hilgenkamp, H. *et al.* Ordering and manipulation of the magnetic moments in large-scale superconducting π-loop arrays. *Nature* **422,** 50–53 (2004).
54. Smilde, H.-J. H., Ariando, Rogalla, H. & Hilgenkamp, H. Bistable superconducting quantum interference device with built-in switchable $\pi/2$ phase shift. *Appl. Phys. Lett.* **85,** 4091–4093 (2003).
55. Taillefer, L., Lussier, B., Gagnon, R., Behnia, K. & Aubin, H. Universal heat conduction in $YBa_2Cu_3O_{6.9}$. *Phys. Rev. Lett.* **79,** 483–486 (1997).
56. Chiao, M. *et al.* Quasiparticle transport in the vortex state of $YBa_2Cu_3O_{6.9}$. *Phys. Rev. Lett.* **82,** 2943–2946 (1999).
57. Turner, P. *et al.* Observation of weak-limit quasiparticle scattering via broadband microwave spectroscopy of a d-wave superconductor. *Phys. Rev. Lett.* **90,** 237005 (2003).
58. Pan, S. H. *et al.* Imaging the effects of individual zinc impurity atoms on superconductivity in $Bi_2Sr_2CaCu_2O_{8+\delta}$. *Nature* **403,** 746–750 (2000).
59. Hudson, E. W. *et al.* Interplay of magnetism and high-T_c superconductivity at individual ni impurity atoms in $Bi_2Sr_2CaCu_2O_{8+\delta}$. *Nature* **411,** 920–924 (2001).
60. Lobb, C. Critical fluctuations in high-T_c superconductors. *Phys. Rev. B* **36,** 3930–3932 (1987).
61. Fisher, D., Fisher, M. & Huse, D. Thermal fluctuations, quenched disorder, phase transitions, and transport in type-II superconductors. *Phys. Rev. B* **43,** 130–159 (1991).
62. Uemura, Y. J. *et al.* Universal correlations between T_c and n_s/m^* (carrier density over effective mass) in high-T_c cuprate superconductors. *Phys. Rev. Lett.* **62,** 2317–2320 (1989).
63. Kamal, S. *et al.* Penetration depth measurements of 3D XY critical behaviour in $YBa_2Cu_3O_{6.95}$ crystals. *Phys. Rev. Lett.* **73,** 1845–1848 (1994).
64. Overend, N., Howson, M. & Lawrie, I. 3D X − Y scaling of the specific heat of $YBa_2Cu_3O_{7-\delta}$ single crystals. *Phys. Rev. Lett.* **72,** 3238–3241 (1994).
65. Pasler, V. *et al.* 3D − XY critical fluctuations of the thermal expansivity in detwinned $YBa_2Cu_3O_{7-\delta}$ single crystals near optimal doping. *Phys. Rev. Lett.* **81,** 1094–1097 (1998).
66. Meingast, C. *et al.* Phase fluctuations and the pseudogap in $YBa_2Cu_3O_{6+x}$. *Phys. Rev. Lett.* **86,** 1606–1609 (2001).
67. Corson, J., Mallozzi, R., Orenstein, J., Eckstein, J. N. & Bozovic, I. Vanishing of phase coherence in underdoped $Bi_2Sr_2CaCu_2O_{8+\delta}$. *Nature* **398,** 221–223 (1999).
68. Wang, Y. *et al.* Field-enhanced diamagnetism in the pseudogap state of the cuprate $Bi_2Sr_2CaCu_2O_{8+\delta}$ superconductor in an intense magnetic field. *Phys. Rev. Lett.* **95,** 247002 (2005).
69. Wang, Y. *et al.* High field phase diagram of cuprates derived from the Nernst effect. *Phys. Rev. Lett.* **88,** 257003 (2002).
70. Wang, Y. *et al.* Dependence of upper critical field and pairing strength on doping in cuprates. *Science* **299,** 86–89 (2002).
71. Shi, J., Ling, X. S., Liang, R., Bonn, D. A. & Hardy, W. N. Giant peak effect observed in an ultrapure $YBa_2Cu_3O_{6.993}$ crystal. *Phys. Rev. B* **60,** 12593–12596 (1999).
72. Farrell, D. E., Rice, J. P. & Ginsberg, D. M. Experimental evidence for flux-lattice melting. *Phys. Rev. Lett.* **67,** 1165–1168 (1991).
73. Liang, R., Bonn, D. A. & Hardy, W. N. Discontinuity of reversible magnetization in untwinned YBCO single crystals at the first order vortex melting transition. *Phys. Rev. Lett.* **76,** 835–838 (1996).
74. Safar, H. *et al.* Experimental evidence for a first-order vortex-lattice-melting transition in untwinned, single crystal $YBa_2Cu_3O_7$. *Phys. Rev. Lett.* **69,** 824–827 (1992).
75. Sonier, J. E., Brewer, J. H. & Kiefl, R. F. μSR studies of the vortex state in type-II superconductors. *Rev. Mod. Phys.* **72,** 769–811 (2000).
76. Malozemoff, A. P., Mannhart, J. & Scalapino, D. High temperature superconductors get to work. *Phys. Today* **58,** 41–47 (2005).
77. Blatter, G., Feigel'man, M. V., Geshkenbein, V. B., Larkin, A. I. & Vinokur, V. M. Vortices in high-temperature superconductors. *Rev. Mod. Phys.* **66,** 1125–1388 (1994).
78. Ruckenstein, A. E., Hirschfeld, P. J. & Appel, J. Mean-field theory of high-T_c superconductivity: the superexchange mechanism. *Phys. Rev. B* **36,** 857–860 (1987).
79. Baskaran, G., Zou, Z. & Anderson, P. W. The resonating valence bond state and high-T_c superconductivity - a mean field theory. *Solid State Comm.* **63,** 973–976 (1987).
80. Emery, V. J. & Kivelson, S. A. Importance of phase fluctuations in superconductors with small superfluid density. *Nature* **374,** 434–437 (1995).
81. Timusk, T. & Statt, B. The pseudogap in high-temperature superconductors: an experimental survey. *Rep. Prog. Phys.* **62,** 61–122 (1999).
82. Tallon, J. & Loram, J. W. The doping dependence of T^* what is the real high-T_c phase diagram? *Physica C* **349,** 53–68 (2001).
83. Boebinger, G. S. *et al.* Insulator-to-metal crossover in the normal state of $La_{2-x}Sr_xCuO_4$ near optimum doping. *Phys. Rev. Lett.* **77,** 5417–5420 (1996).
84. Lake, B. *et al.* Antiferromagnetic order induced by an applied magnetic field in a high-temperature superconductor. *Nature* **415,** 299–302 (2002).
85. Lake, B. *et al.* Three-dimensionality of field-induced magnetism in a high-temperature superconductor. *Nature Mater.* **4,** 658–662 (2005).
86. Miller, R. I. *et al.* Evidence for static magnetism in the vortex cores of ortho-II $YBa_2Cu_3O_{6.50}$. *Phys. Rev. Lett.* **88,** 137002 (2002).
87. Maggio-Aprile, I., Renner, C., Erb, A., Walker, E. & Fischer, Ø. Direct vortex lattice imaging and tunneling spectroscopy of flux lines on $YBa_2Cu_3O_{7-\delta}$. *Phys. Rev. Lett.* **75,** 2754–2757 (1995).
88. Hoffman, J. E. *et al.* A four unit cell periodic pattern of quasi-particle states surrounding vortex cores in $Bi_2Sr_2CaCu_2O_{8+\delta}$. *Science* **295,** 466–469 (2002).
89. Hanaguri, T. *et al.* A checkerboard electronic crystal state in lightly hole-doped $Ca_{2-x}Na_xCuO_2Cl_2$. *Nature* **430,** 1001–1005 (2004).
90. McElroy, K. *et al.* Atomic-scale sources and mechanism of nanoscale electronic disorder in $Bi_2Sr_2CaCu_2O_{8+\delta}$. *Science* **309,** 1048–1052 (2005).
91. Corson, J., Orenstein, J., Oh, S., O'Donnell, J. & Eckstein, J. N. Nodal quasiparticle lifetime in the superconducting state of $Bi_2Sr_2CaCu_2O_{8+\delta}$. *Phys. Rev. Lett.* **85,** 2569–2572 (2000).
92. Breit, V. *et al.* Evidence for chain superconductivity in near-stoichiometric $YBa_2Cu_3O_x$ single crystals. *Phys. Rev. B* **52,** 15727–15730 (1995).
93. Eisaki, H. *et al.* Effect of chemical inhomogeneity in bismuth-based copper oxide superconductors. *Phys. Rev. B* **69,** 064512 (2004).
94. Feng, D. L. *et al.* Electronic excitations near the brillouin zone boundary of $Bi_2Sr_2CaCu_2O_{8+\delta}$. *Phys. Rev. B* **65,** 220501 (2002).

Acknowledgements

The author would like to thank D. Peets, Z.-X. Shen, H. Hilgenkamp, C. Meingast and K. McElroy for providing figures. This manuscript owes a debt to the thoughts of countless fellow researchers over twenty years, but I am particularly grateful to W. N. Hardy and Ruixing Liang.
Correspondence and requests for materials should be addressed to D.A.B.

Competing financial interests

The authors declare that they have no competing financial interests.